Genuine Many-Body Quantum Scars along Unstable Modes in Bose-Hubbard Systems

Quirin Hummel,[1,2] Klaus Richter,[2] and Peter Schlagheck[1]
[1]CESAM research unit, University of Liege, B-4000 Liège, Belgium
[2]Institut für Theoretische Physik, Universität Regensburg, D-93040 Regensburg, Germany

(Received 22 December 2022; accepted 30 May 2023; published 21 June 2023)

The notion of many-body quantum scars is associated with special eigenstates, usually concentrated in certain parts of Hilbert space, that give rise to robust persistent oscillations in a regime that globally exhibits thermalization. Here we extend these studies to many-body systems possessing a true classical limit characterized by a high-dimensional chaotic phase space, which are not subject to any particular dynamical constraint. We demonstrate genuine quantum scarring of wave functions concentrated in the vicinity of unstable classical periodic mean-field modes in the paradigmatic Bose-Hubbard model. These peculiar quantum many-body states exhibit distinct phase-space localization about those classical modes. Their existence is consistent with Heller's scar criterion and appears to persist in the thermodynamic long-lattice limit. Launching quantum wave packets along such scars leads to observable long-lasting oscillations, featuring periods that scale asymptotically with classical Lyapunov exponents, and displaying intrinsic irregularities that reflect the underlying chaotic dynamics, as opposed to regular tunnel oscillations.

DOI: 10.1103/PhysRevLett.130.250402

The past decade has witnessed tremendous progress in the understanding of the key mechanisms that inhibit thermalization in complex quantum many-body systems. While many-body localization generically arises in the presence of a significant amount of disorder and/or interaction [1–5], nongeneric phenomena of weak ergodicity breaking, typically manifested by persistent oscillatory behavior of observables [6], can occur in systems that globally exhibit eigenstate thermalization in the considered parameter regime. Such ergodicity breaking behavior is generally attributed to *scarring* [7], a concept that was originally introduced in single-particle chaotic quantum systems exhibiting two degrees of freedom [8,9]. A scar in the proper sense refers to a quantum eigenstate that is semiclassically anchored on an unstable periodic orbit [8,9] instead of being equidistributed over the entire chaotic phase space as predicted by the eigenstate thermalization hypothesis [10,11]. As argued by Heller [8], such a scarred eigenstate can exist provided the period T of the orbit is relatively short and its Lyapunov exponent λ relatively weak, i.e., $T\lambda \lesssim 2\pi$, such that a wave packet that is launched along this orbit will almost recover its original shape after one period. Scars are not to be confused with ordinary "regular" quantum states anchored on stable periodic orbits, whose existence and characteristics are most straightforwardly inferred from Einstein-Brillouin-Keller quantization rules [12].

The recent discovery of many-body scars in quantum simulators [6,13], followed by numerous theoretical studies employing spin chains, PXP models, or dynamically constrained systems (e.g. [7,14–24], see [25–27] for recent reviews), calls for an investigation of those scar characteristics in the high dimensional domain. In the context of the widely considered spin-chain-like systems such a study is, however, hampered by the fact that those quantum Hamiltonians do not have an obvious classical counterpart that would naturally arise from a semiclassical evaluation of Feynman's path integral [28]. Artificial classical phase spaces can nevertheless be constructed using the time-dependent variational principle [18], by which means unstable periodic orbits associated with many-body scars can indeed be identified.

To extend the investigations of many-body scars to quantum systems possessing a true classical (chaotic) limit, we propose here to study many-body scars in Bose-Hubbard (BH) systems, whose high-dimensional classical counterpart is well defined and given in terms of a discrete nonlinear Schrödinger equation. Unlike other recent studies on scarring in BH systems [21–23], we shall not consider a dynamically constrained configuration owing to the presence of correlated hopping, periodic driving, or tilting, but study unconstrained homogeneous rings of finite size, square plaquettes in particular. The scars that we find there are anchored on unstable classical staggered dimer configurations, for which the exchange of population between adjacent lattice sites is dynamically suppressed despite nonvanishing hopping matrix elements. As is shown in Fig. 1, a preparation of a quantum state on such a classical configuration gives rise to persistent oscillatory behavior in one-body observables, indicating the absence of thermalization. Irregular features are identified in these oscillations [panels (a),(b)], in line with the high dimensionality of the underlying chaotic phase space in which the dynamics takes place.

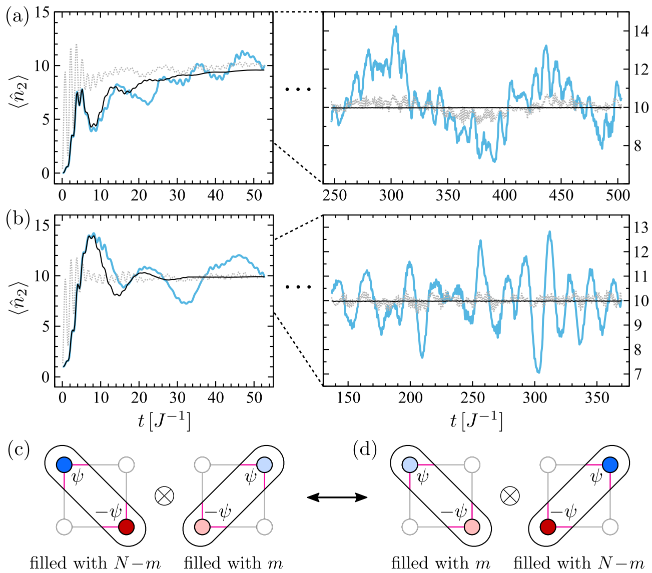

FIG. 1. Persistent oscillations reflecting quantum chaotic scarring. (a),(b): time evolution of the on-site occupancy $\langle \hat{n}_2 \rangle$. When initialized in staggered dimer product states $|\pi_m\rangle$ [see Eq. (9)] the system oscillates [blue lines, with (a) $m = 0$ and (b) $m = 2$] between coupled partners (c) $|\pi_m\rangle$ and (d) $|\pi_{N-m}\rangle$, symmetry-related by 90° rotation of the plaquette. In contrast, classical dynamics (as implemented by TWA, black) as well as quantum evolution of initial Fock states $|[(N-m)/2], (m/2), [(N-m)/2], (m/2)\rangle$ (dotted gray) undergo fast thermalization (for particle number $N = 40$ and effective interaction $\gamma = 0.95$).

We consider N interacting bosonic particles confined to a one-dimensional periodic lattice of L wells. This system is described by the BH Hamiltonian

$$\hat{H} = -J \sum_{l=1}^{L} (\hat{a}_{l+1}^\dagger \hat{a}_l + \hat{a}_l^\dagger \hat{a}_{l+1}) + \frac{U}{2} \sum_{l=1}^{L} \hat{n}_l(\hat{n}_l - 1) \quad (1)$$

with bosonic on-site creation, annihilation, and number operators $\hat{a}_l^\dagger$, $\hat{a}_l$, and $\hat{n}_l = \hat{a}_l^\dagger \hat{a}_l$, where we have nearest-neighbor hopping J, repulsive on-site interaction $U > 0$, and periodic boundary conditions, $l \in \mathbb{Z}_L$. It formally admits a well-defined classical limit where the system is described by a condensate wave function $\boldsymbol{\psi} = (\psi_1, \ldots, \psi_L) \in \mathbb{C}^L$ whose time evolution is governed by the discrete nonlinear Schrödinger equation (DNLSE)

$$i\dot{\psi}_l = -J(\psi_{l-1} + \psi_{l+1}) + U(\psi_l^* \psi_l - 1)\psi_l \quad (2)$$

(setting $\hbar = 1$). The latter is obtained as the saddle point equation in the path integral formulation of the quantum system [29–31], yielding the quantum-to-classical mappings $\hat{a}_l \mapsto \psi_l$, $\hat{a}_l^\dagger \mapsto \psi_l^*$, and $\hat{n}_l + 1/2 = (\hat{a}_l \hat{a}_l^\dagger + \hat{a}_l^\dagger \hat{a}_l)/2 \mapsto |\psi_l|^2$. As a purely classical description, Eq. (2) becomes formally valid in the mean-field regime of large average site occupancies $N/L \to \infty$ and small $U \to 0$, scaled such that the effective dimensionless interaction parameter

$$\gamma = (N/L + 1/2)U/J \quad (3)$$

is kept fixed. Up to a scaling of the time t and a constant shift in energy, γ is the only parameter of the DNLSE.

We now focus on site numbers L that are multiples of four. In that case, the *staggered dimer* configuration, generally characterized by a wave function of the form

$$\boldsymbol{\psi} = (\psi_1, \psi_2, -\psi_1, -\psi_2, \psi_1, \psi_2, -\psi_1, -\psi_2, \ldots) \quad (4)$$

for a pair of complex amplitudes ψ_1, ψ_2, represents a fixed point of the site occupancies in the framework of the classical DNLSE (2). Despite a nonzero $J > 0$, hopping is dynamically suppressed in this configuration, and the site amplitudes ψ_l feature only phase oscillations with frequencies $\omega_l = U(n_l - 1)$ at constant $n_l = |\psi_l(0)|^2$. While this resembles the Mott-insulator physics of $U/J \to \infty$, it is here a result of a fragile balance, crucially depending on the equal populations and relative phase of π between next-nearest neighbors. A slight deviation from the staggered-dimer manifold $\mathcal{M}_{\mathrm{SD}}$, given by all $\boldsymbol{\psi}$ of the form (4), breaks this balance, leading to population transfer that may further push the system away from this manifold. As a result, staggered dimer waves are, in a wide parameter range, at the same time fundamental short and unstable periodic modes, thus representing excellent candidates for scarring.

Semiclassically, the phenomenon of scarring is generally described as concentration of particular eigenstates of the Hamiltonian along unstable periodic orbits of the corresponding classical system that are at least locally embedded in a patch of chaotic motion. In the present context, "periodicity" of a mean-field solution has to be understood modulo a global phase, i.e., we call $\boldsymbol{\psi}(t)$ *periodic* with period T if for some (irrelevant) $\theta \in \mathbb{R}$

$$\boldsymbol{\psi}(t + T) = \boldsymbol{\psi}(t) e^{i\theta}. \quad (5)$$

To test whether a given state is scarred by such a periodic orbit $\boldsymbol{\psi}(t)$, or, more generically, by a family of such orbits defined in a finite range of energy, we employ so-called tube states [32,33] constructed as

$$|\mathcal{T}_{\boldsymbol{\psi}(t)}\rangle \equiv \mathcal{N} \int_0^T dt\, e^{i[S(t) - \pi\mu(t)/2]} |\boldsymbol{\psi}(t)\rangle_N. \quad (6)$$

Here we define the number-projected coherent state

$$|\boldsymbol{\psi}\rangle_N = \frac{1}{\sqrt{N!}} (\mathbf{e}_{\boldsymbol{\psi}} \cdot \boldsymbol{a}^\dagger)^N |0\rangle \propto \hat{\Pi}_N e^{\boldsymbol{\psi} \cdot \boldsymbol{a}^\dagger} |0\rangle \quad (7)$$

centered about the phase-space point $\boldsymbol{\psi}$, with $\mathbf{e}_{\boldsymbol{\psi}} \equiv \boldsymbol{\psi}/\sqrt{\boldsymbol{\psi} \cdot \boldsymbol{\psi}^*}$, $|0\rangle$ the vacuum state, and $\hat{\Pi}_N$ the projector to the N-particle sector. These tube states are forced to be concentrated along the trajectory by placing a wave packet $|\boldsymbol{\psi}(t)\rangle_N$ at each of its points. The dressing with a phase factor determined by classical dynamics, containing the accumulated classical action S and Maslov index μ, ensures constructive interference of neighboring wave packets and is here especially devised for oscillatorlike systems [34]. Demanding the wave packets at $t = 0$ and after time T to be in phase gives the Bohr-Sommerfeld (BS) type quantization condition

$$S(T) - \pi\mu(T)/2 + N\theta \equiv 0 \pmod{2\pi}, \qquad (8)$$

singling out a discrete set of quantized orbits and corresponding tube states for each family of periodic orbits.

To ease discussions, we first focus on the simplest case $L = 4$, corresponding to a single square plaquette, and thus consider the manifold of staggered dimers given by condensate wave functions of the form $\boldsymbol{\psi} = (\psi_1, \psi_2, -\psi_1, -\psi_2)$. Then the above semiclassical construction yields quantized tube states (6) with an intriguing structure. Specifically, one finds that the mth quantized staggered dimer tube state $|\mathcal{T}_m\rangle$, $m \in \{0, \ldots, N\}$, starting with maximal population of sites $l = 1, 3$ at $m = 0$, is very well described by a product state of the form

$$|\mathcal{T}_m\rangle \simeq |\pi_m\rangle \equiv |(\psi_1, -\psi_1)\rangle^{(1,3)}_{N-m} \otimes |(\psi_2, -\psi_2)\rangle^{(2,4)}_{m}. \qquad (9)$$

The two factors are states (7) on the Hilbert subspaces living on sites (1, 3) and (2, 4), respectively [see Figs. 1(c) and 1(d)]. As a direct product of number states on disjoint subspaces, the states (9) do not show any phase coherence between the two diagonals (1, 3) and (2, 4), as is classically evident from the different phase velocities ω_1 and ω_2, whereas the phase relation between the two opposite sites within each diagonal is fixed to π.

A characteristic hallmark for the existence of many-body scars anchored on staggered dimers can indeed be found by the numerical propagation of quantum many-body wave packets that are initialized on the states (9). As shown in Fig. 1, persistent oscillations, displaying no decay over very long time scales (blue lines), arise in the mean site occupancies, in contrast to classical simulations based on the truncated Wigner approximation (TWA) that would predict rapid relaxation to thermal equilibrium (black). Note that such a relaxation behavior would also occur (gray) if the wave packet was initialized on a Fock state $|\nu_1, \nu_2, \nu_1, \nu_2\rangle$ having the same mean site occupancies $\nu_1 = (N - m)/2$ and $\nu_2 = m/2$ as the state (9). This demonstrates the importance of the specific structure of the staggered dimer states for the occurrence of scarring.

Further confirmation for the existence of genuine quantum scarring on staggered dimers is obtained via several (semi-)classical indicators, which are evaluated in Fig. 2 as functions of the imbalance $z = (n_1 - n_2)/(n_1 + n_2)$. For the chosen intermediate coupling $\gamma = 0.95$, Eq. (3), we find that quantum scars are likely to occur, independently of N, for imbalances $z \gtrsim z^*$ with $z^* \simeq 0.33$ (dotted vertical line),

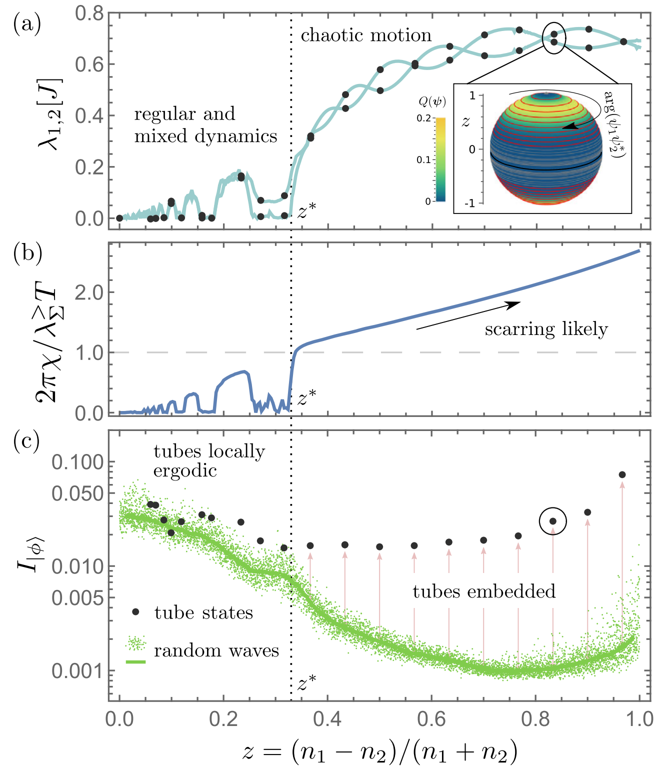

FIG. 2. Indicators for scarring. (a) Dominant stability exponents, $\lambda_{1,2} \geq 0$, along the staggered-dimer manifold. Central orbits of Bohr-Sommerfeld (BS)-quantized tubes are marked by dots. Inset: Husimi section of one quantized tube $\mathcal{T}_2^-$ in the manifold mapped to a Bloch sphere. (b) Heuristic rating for the likelihood of quantum scarring based on the Heller criterion (see text). (c) Inverse participation ratio (10) of BS-quantized tube states (black dots) and random-wave states (green dots) on local constant-energy layers (see text). As a guide to the eye, a running median is added (solid green).

where dynamics is chaotic as indicated by Fig. 2(a). The likelihood for scarring increases when approaching the maximally imbalanced limit due to ever shorter periods T. This is demonstrated in Fig. 2(b), where we use an *a priori* indicator $2\pi\chi/\lambda_\Sigma^+ T > 1$ for periodic orbits to support quantum scars, generalizing the heuristic Heller criterion [8] for two-dimensional single-particle systems [34,35]. Here, $\lambda_\Sigma^+ \equiv \Sigma_j^> \lambda_j$ is the sum of positive stability exponents, and $\chi \equiv \prod_j^> 2\lambda_j/(\lambda_{\mathrm{th}} + \lambda_j)$ is a heuristic factor to suppress close-to-regular or mixed dynamics with a threshold chosen as $\lambda_{\mathrm{th}} = 0.3J$.

Additionally, we investigate in Fig. 2(c) the phase-space localization of the corresponding tube states by means of the phase-space inverse participation ratio (IPR)

$$I_{|\phi\rangle} \equiv \mathcal{N} \int d^{2L}\psi\, \delta(\|\boldsymbol{\psi}\|^2 - L/2 - N) Q_{|\phi\rangle}(\boldsymbol{\psi})^2 \qquad (10)$$

of a state $|\phi\rangle$, defined in terms of the Husimi function $Q_{|\phi\rangle}(\boldsymbol{\psi}) \equiv |\langle\phi|\boldsymbol{\psi}\rangle_N|^2$. We compare the IPR of tube states to the one of random-wave states spread across the local layers of constant energy in which the corresponding relevant orbits are embedded. These locally ergodic states are obtained similar to the tubes (6) but with slightly perturbed initial conditions, putting wave packets $|\boldsymbol{\psi}(t)\rangle_N$ with random phases after finite time steps $dt \mapsto \Delta t$ and following the classical dynamics long enough to saturate the local constant-energy surface. While in the regime $z \lesssim z^*$ of mixed regular and chaotic dynamics the tubes are found to fill up thin constant-energy layers alike random waves, they are, as seen in Fig. 2(c), significantly more localized than the latter in the dominantly chaotic regime $z > z^*$, thereby confirming their nonclassical scarlike nature [36].

To confirm the existence of actual quantum scarring of staggered dimer solutions, we perform exact diagonalization and examine all individual eigenstates for their phase-space localization and overlap with tube states. Figure 3 shows again the case $\gamma = 0.95$, for which the energy range relevant for staggered dimers lies in the central spectrum of highly excited states, as indicated by the highlighted region of the inset. We focus on the subspectra with the symmetry $(+,+)$, denoting fully even parity with respect to the two diagonal exchange operations (sites $1 \leftrightarrow 3$ as well as $2 \leftrightarrow 4$) of the plaquette. For even particle number N this

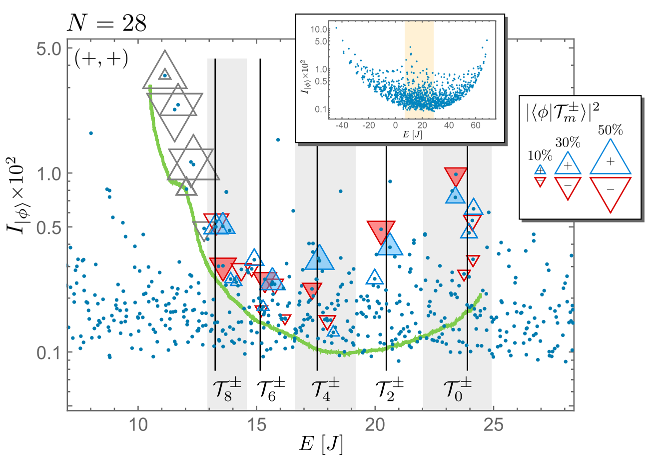

FIG. 3. Phase-space localization of eigenstates as measured by the IPR (10) for $\gamma = 0.95$ and $N = 28$ in the central energy range where staggered dimer waves are located [highlighted regions in the full-range spectra $(+,+)$ shown as inset]. The overlap $|\langle\phi|\mathcal{T}_m^\pm\rangle|^2$ of eigenstates $|\phi\rangle$ with the symmetric and antisymmetric tube states, whenever greater than 0.1, is indicated by the size of triangles pointing up and down, respectively. In the unstable regime $z \gtrsim z^*$, these are shown in blue and red, respectively, with shading marking the eigenstates that have the largest overlap with the respective tube states $\mathcal{T}_{0,2,4,6,8}^\pm$ (regular states, for $z < z^*$, are shown in gray without shading). Vertical lines mark the energies of quantized orbits. Locally ergodic random waves about $\mathcal{M}_{\mathrm{SD}}$ are shown as the running median in green [see Fig. 2(c)].

symmetry class is shared by the staggered dimer tube states of *even* BS quantization index m [odd m gives tube states of odd parity $(-,-)$]. We find a small number of eigenstates that are anomalously localized as compared to the majority of eigenstates with comparable energy. As confirmed by strong overlaps with tube states, a big part of these can be directly identified as a class of staggered-dimer-like states. Apart from some genuinely "regular" states featuring a high IPR due to localization on classically stable phase-space structures (which are, hence, not scars according to the definition of this concept [8]), this class also contains eigenstates that are strongly concentrated along *unstable* staggered-dimer solutions embedded in *chaotic* portions of the phase space. Since their number scales proportionally to N as does the number of tube states (9), they constitute a vanishing fraction of the full spectra with Hilbert-space dimension $\sim N^{L-1}$ as $N \to \infty$. We thus find all criteria for genuine quantum scarring fulfilled. Note that even in the deep quantum regime of very few particles, where quantum-to-classical correspondence is no longer expected to hold, we can unambiguously identify *direct descendants* of genuine quantum scars by maintaining the link between tube states and eigenstates while successively lowering N [34].

Let us discuss the absence of regularity in the oscillatory behavior of the mean site occupancies, shown in Fig. 1. They oscillate due to the (anti-)symmetry of eigenstates with respect to the rotation of the lattice by one site, induced by the operator $\hat{R}_1$, such that scar states in the Hamiltonian's eigenspectrum exhibit a strong overlap with the two linear combinations $|\mathcal{T}_m^\pm\rangle \propto (1 \pm \hat{R}_1)|\mathcal{T}_m\rangle$. Hence, the preparation of the quantum system on a staggered-dimer state with broken symmetry, such as $|\mathcal{T}_m\rangle$, is expected to give rise to Rabi-like oscillations between $|\mathcal{T}_m\rangle$ and $\hat{R}_1|\mathcal{T}_m\rangle$, with a frequency that corresponds to the level splitting of the two eigenstates $|\mathcal{T}_m^\pm\rangle$. This simplified reasoning is to be amended due to the fact that several eigenstates can generally be scarred with the same orbit [8,33]. An initial product state $|\pi_m\rangle$ gives thus rise to a superposition of corresponding frequencies and amplitudes, resulting in beatings that do not feature a clean harmonic behavior. In a semiclassical picture, the beating period can be estimated to be related to the classical rate to leave (or approach) the vicinity of one of these orbits, i.e., to be proportional to their inverse stability exponents λ_j [37]. We confirm this scaling for the regime of weak to moderate interactions [34] where all classical stability exponents tend to be equal to a unique Lyapunov exponent, $\lambda_j \simeq \lambda_L$, such that a uniform time scale $\sim\lambda_L^{-1}$ emerges. Most notably, this oscillatory behavior is in stark contrast to the more pronounced and regular oscillations that one finds in a regime of locally *stable* or close-to-stable classical dynamics, where by definition scars cannot occur [34].

Scarring on the staggered dimer configuration (4) is not restricted to the four-site plaquette but can be found also for larger systems [34], such as the $L = 8$ site BH ring, where scars are anchored on wave functions of the form $|(\psi_1, -\psi_1, \psi_1, -\psi_1)\rangle_{N-m}^{(1,3,5,7)} \otimes |(\psi_2, -\psi_2, \psi_2, -\psi_2)\rangle_m^{(2,4,6,8)}$, as well as the $L = 12$ site ring. In both cases, similar irregular long-period oscillations are encountered as for the four-site plaquette [34]. The staggered-dimer modes in those high-L BH rings are found to have very similar Lyapunov exponents $\lambda_j \sim \gamma J$ and periods $T \sim \pi/\gamma J$, yielding a γ-independent Heller-type indicator $2\pi/\lambda_\Sigma^+ T \sim 2/(L-2)$ that scales inversely with the number of chaotic degrees of freedom transverse to the mode. This would *a priori* predict a decreasing likelihood for the existence of staggered-dimer scars with increasing L. However, we expect this effect to be counterbalanced by the increasing number $\nu = L/4$ of discrete rotational symmetries that staggered dimer configurations feature. The associated quantum states live in the corresponding symmetry subspaces whose dimensions are consequently lowered by a factor $\propto 1/L$ with respect to the full Hilbert space and which thus exhibit a reduced density of states as compared to the latter. This reduction factor is expected [34] to effectively enhance the otherwise deficient Heller-type indicator to a sufficient extent, yielding support for the existence of staggered dimer scars in the thermodynamic long-lattice limit; see, e.g., scarring within a 1.35×10^6-dimensional Hilbert space in the specific case of a $L = 12$ site BH ring [34].

In summary, we present solid evidence for the existence of genuine scars in a preeminent bosonic many-body system that is not subject to any dynamical constraint, namely, a homogeneous disorder-free BH ring. These scars form in the vicinity of the classical staggered dimer configuration (4) where population exchange between sites is dynamically suppressed despite a nonvanishing hopping parameter. The time evolution of quantum states launched on such staggered dimers reveals an intriguing feature that we conjecture to be generic for many-body scars in a high-dimensional chaotic phase space, namely, the existence of persistent long-period oscillations that do not exhibit a well identifiable regularity. This feature is open to experimental verification within state-of-the-art quantum simulators employing ultracold bosonic atoms in optical lattices [5]. There, staggered-dimer product states (9) can be created by quantum quenches starting, e.g., from spatially separated left- and right-diagonal sublattices that are brought together at $t = 0$ to form the plaquette. We believe that scarring is a generic phenomenon in high-dimensional bosonic many-body systems exhibiting chaotic dynamics, and our study lays proper foundations for their unambiguous identification and characterization.

We are grateful for inspiring discussions with Steven Tomsovic, Denis Ullmo, and Juan Diego Urbina. This research was supported by the University of Liège under Special Funds for Research, IPD-STEMA Programme, and by the Deutsche Forschungsgemeinschaft through Project No. Ri681/15-1 within the Reinhart-Koselleck Programme.

[1] I. V. Gornyi, A. D. Mirlin, and D. G. Polyakov, Phys. Rev. Lett. **95**, 206603 (2005).
[2] D. Basko, I. Aleiner, and B. Altshuler, Ann. Phys. (Amsterdam) **321**, 1126 (2006).
[3] V. Oganesyan and D. A. Huse, Phys. Rev. B **75**, 155111 (2007).
[4] M. Žnidarič, T. Prosen, and P. Prelovšek, Phys. Rev. B **77**, 064426 (2008).
[5] A. Lukin, M. Rispoli, R. Schittko, M. E. Tai, A. M. Kaufman, S. Choi, V. Khemani, J. Léonard, and M. Greiner, Science **364**, 256 (2019).
[6] H. Bernien, S. Schwartz, A. Keesling, H. Levine, A. Omran, H. Pichler, S. Choi, A. S. Zibrov, M. Endres, M. Greiner, V. Vuletić, and M. D. Lukin, Nature (London) **551**, 579 (2017).
[7] C. J. Turner, A. A. Michailidis, D. A. Abanin, M. Serbyn, and Z. Papić, Nat. Phys. **14**, 745 (2018).
[8] E. J. Heller, Phys. Rev. Lett. **53**, 1515 (1984).
[9] E. B. Bogomolny, Physica (Amsterdam) **31D**, 169 (1988).
[10] J. M. Deutsch, Phys. Rev. A **43**, 2046 (1991).
[11] M. Srednicki, Phys. Rev. E **50**, 888 (1994).
[12] M. V. Berry and M. Tabor, Proc. R. Soc. A **349**, 101 (1976).
[13] D. Bluvstein, A. Omran, H. Levine, A. Keesling, G. Semeghini, S. Ebadi, T. T. Wang, A. A. Michailidis, N. Maskara, W. W. Ho, S. Choi, M. Serbyn, M. Greiner, V. Vuletić, and M. D. Lukin, Science **371**, 1355 (2021).
[14] S. Moudgalya, N. Regnault, and B. A. Bernevig, Phys. Rev. B **98**, 235156 (2018).
[15] M. Schecter and T. Iadecola, Phys. Rev. Lett. **123**, 147201 (2019).
[16] S. Chattopadhyay, H. Pichler, M. D. Lukin, and W. W. Ho, Phys. Rev. B **101**, 174308 (2020).
[17] J.-Y. Desaules, A. Hudomal, C. J. Turner, and Z. Papić, Phys. Rev. Lett. **126**, 210601 (2021).
[18] W. W. Ho, S. Choi, H. Pichler, and M. D. Lukin, Phys. Rev. Lett. **122**, 040603 (2019).
[19] V. Khemani, C. R. Laumann, and A. Chandran, Phys. Rev. B **99**, 161101(R) (2019).
[20] S. Choi, C. J. Turner, H. Pichler, W. W. Ho, A. A. Michailidis, Z. Papić, M. Serbyn, M. D. Lukin, and D. A. Abanin, Phys. Rev. Lett. **122**, 220603 (2019).
[21] A. Hudomal, I. Vasić, N. Regnault, and Z. Papić, Commun. Phys. **3**, 99 (2020).
[22] H. Zhao, J. Vovrosh, F. Mintert, and J. Knolle, Phys. Rev. Lett. **124**, 160604 (2020).
[23] G.-X. Su, H. Sun, A. Hudomal, J.-Y. Desaules, Z.-Y. Zhou, B. Yang, J. C. Halimeh, Z.-S. Yuan, Z. Papić, and J.-W. Pan, Phys. Rev. Res. **5**, 023010 (2023).
[24] A. Hudomal, J.-Y. Desaules, B. Mukherjee, G.-X. Su, J. C. Halimeh, and Z. Papić, Phys. Rev. B **106**, 104302 (2022).
[25] M. Serbyn, D. A. Abanin, and Z. Papić, Nat. Phys. **17**, 675 (2021).

[26] Z. Papić, in *Entanglement in Spin Chains—From Theory to Quantum Technology Applications*, edited by A. Bayat, S. Bose, and H. Johannesson (Springer, New York, 2022).

[27] S. Moudgalya, B. A. Bernevig, and N. Regnault, Rep. Prog. Phys. **85**, 086501 (2022).

[28] M. C. Gutzwiller, *Chaos in Classical and Quantum Mechanics* (Springer, New York, 1990).

[29] T. Engl, J. Dujardin, A. Argüelles, P. Schlagheck, K. Richter, and J. D. Urbina, Phys. Rev. Lett. **112**, 140403 (2014).

[30] R. Dubertrand and S. Müller, New J. Phys. **18**, 033009 (2016).

[31] K. Richter, J. D. Urbina, and S. Tomsovic, J. Phys. A **55**, 453001 (2022).

[32] E. G. Vergini, Phys. Rev. Lett. **108**, 264101 (2012).

[33] F. Revuelta, E. G. Vergini, R. M. Benito, and F. Borondo, Phys. Rev. E **85**, 026214 (2012).

[34] See Supplemental Material at http://link.aps.org/supplemental/10.1103/PhysRevLett.130.250402 for details on the tube state construction (A), the multidimensional generalization of Heller's criterion (B), quantum scarring when approaching low N (C), the emergence of a uniform time scale (D), the comparison with regular tunnelling oscillations in the self-trapping regime (E), and quantum scarring in larger chains (F).

[35] Q. Hummel and P. Schlagheck, J. Phys. A **55**, 384009 (2022).

[36] In principle, minor chaotic layers in the mixed regime, e.g., for $0.2 \lesssim z \lesssim 0.25$ in Figs. 2(a) and 2(b), may also be able to host quantum scars for sufficiently large total particle number N. For all investigated parameters, however, a clear characterization of tube states as strongly embedded within locally ergodic patches by means of Eq. (10) was only possible for the steadily chaotic regime $z \gtrsim z^*$.

[37] Q. Hummel, B. Geiger, J. D. Urbina, and K. Richter, Phys. Rev. Lett. **123**, 160401 (2019).